

Synergistic antitumor efficacy of antibacterial helvolic acid from *Cordyceps taii* and cyclophosphamide in a tumor mouse model

Jian-Hui Xiao^{1,*}, Yao Zhang¹, Gui-You Liang¹, Ru-Ming Liu¹, Xiao-Gang Li¹, Ling-Tao Zhang¹, Dai-Xiong Chen¹ and Jian-Jiang Zhong^{2,*}

¹Centre for Translational Medicinal of Guizhou Province, Affiliated Hospital of Zunyi Medical University, Zunyi 563000, PR China; ²State Key Laboratory of Microbial Metabolism, and School of Life Science & Biotechnology, Shanghai Jiao Tong University, Shanghai 200240, PR China

*Corresponding authors: Jian-Hui Xiao. Email: jianhuixiao@126.com; Jian-Jiang Zhong. Email: jjzhong@sjtu.edu.cn

Abstract

The antibacterial agent helvolic acid, which was isolated from the active antitumor fraction of *Cordyceps taii*, showed potent cytotoxicity against different human cancer cells. In the present study, the *in vivo* antitumor effect of helvolic acid was investigated in murine sarcoma S180 tumor-bearing mice. Doses of 10 and 20 mg/kg/day helvolic acid did not exert significant antitumor activity. Interestingly, co-administration of 10 mg/kg/day helvolic acid and 20 mg/kg/day cyclophosphamide (CTX) – a well-known chemotherapy drug – showed promising antitumor activity with a growth inhibitory rate of 70.90%, which was much higher than that of CTX alone (19.5%). Furthermore, the combination markedly prolonged the survival of tumor-bearing mice. In addition, helvolic acid enhanced the immune organ index. The protein expression levels of β -catenin, cyclin D1, and proliferating cell nuclear antigen were significantly suppressed in mice treated with 20 mg/kg/day helvolic acid and in those receiving combination therapy. Taken together, these results indicated that helvolic acid in combination with CTX showed potent *in vivo* synergistic antitumor efficacy, and its mechanism of action may involve the Wnt/ β -catenin signaling pathway.

Keywords: Medicinal mushroom, *Cordyceps taii*, helvolic acid, antitumor activity, synergistic effect, cyclophosphamide, mechanism of action

Experimental Biology and Medicine 2017; 242: 214–222. DOI: 10.1177/1535370216668051

Introduction

Helvolic acid, a naturally occurring antibacterial nortriterpenoid that is also called fumigacin, was isolated from the culture filtrates of an opportunistic pathogen, *Aspergillus fumigatus*. Recent studies showed that it was present in different fungi including *Pichia guilliermondii*, *Xylaria* spp., and *Metarhizium anisopliae*.^{1–3} Helvolic acid has a wide spectrum of antibacterial activity^{1–4} and exhibits a potent synergistic effect with erythromycin against multi-drug resistant *Staphylococcus aureus*.⁵ This therapeutic potential has been explored in extensive chemical and biological studies.^{2,6,7} Recently, our research group found that two *Cordyceps* species, *Cordyceps jiangxiensis* and *Cordyceps taii*, also produced helvolic acid,^{8,9} and that *C. taii* showed a broad-spectrum antimicrobial activity,^{10,11} for which helvolic acid may be partially responsible. Interestingly, helvolic acid was isolated and identified from the active antitumor fraction of *C. taii*,¹² therefore the antitumor activity of helvolic acid was subsequently evaluated *in vitro* by our group, where it exhibited notable cytotoxicity against different human

cancer cell lines including those originating from the pancreas, liver, cervix, and lung (SW1990, HepG2, HeLa, and 95-D cell lines, respectively). In particular, it showed a two-fold higher activity than a first-line chemotherapeutic agent, hydroxycamptothecin.¹³ These findings suggest that helvolic acid may produce antitumor effects *in vivo*. However, the antitumor potential of helvolic acid has not been fully investigated using *in vivo* animal models.

Sarcoma 180 (S180) is an original mouse tumor and one of the most frequently used cancer cell lines in the evaluation of the antitumor agents due to its transplantable, and well-characterized experimental model.^{12,14–17} Therefore, the present study used a S180 tumor-bearing mouse model to investigate the antitumor effect of helvolic acid *in vivo* and to explore the possible mechanisms underlying this effect.

Cyclophosphamide, also known as cytophosphane, is a medication mainly used in chemotherapy that works by inducing the death of certain T cells. It is an alkylating agent of the nitrogen mustard type, specifically the oxazaphosphorine group. As a chemotherapy drug, its main use

is with other chemotherapy agents in the treatment of lymphomas, some forms of brain cancer, leukemia as well as some solid tumors. In this work, the possible synergistic antitumor efficacy of *Cordyceps*-derived helvolic acid and cyclophosphamide was explored in a tumor mouse model.

Materials and methods

Reagents

The primary antibodies against proliferating cell nuclear antigen (PCNA), β -catenin, and cyclin D1, as well as the horseradish peroxidase-conjugated secondary IgG antibodies, were from Abcam (Cambridge, UK). The Roswell Park Memorial Institute (RPMI)-1640 culture medium, fetal bovine serum (FBS), GlutaMAX, and HEPES were from Gibco (Invitrogen Life Technologies, NY, USA). The castor oil for injection, Tween-80, and dimethyl sulfoxide (DMSO) were from Sigma-Aldrich (St. Louis, MO, USA), while the cyclophosphamide (CTX) for injection was purchased from Jiangsu Hengrui Medicine Co., Ltd (Lot No. 14012225, Lianyungang, China). All other reagents were from China, unless otherwise specified.

Preparation and identification of helvolic acid

The helvolic acid was prepared using previously described methods.^{9,18} Briefly, the dried mycelia powder of *C. taiti* (4400 g) was extracted by soaking it in cold 70% ethanol (25 L) six times for 8 h each time, and a brown crude extract (1200 g) was obtained. The extract was resuspended in hot water and extracted three times with equal volumes of chloroform (CHCl₃). The organic layer was evaporated under reduced pressure to yield a brown chloroform extract (142 g), which was subjected to column chromatography using silica gel, and eluted with a CHCl₃-methanol (MeOH; 100:0-100:0, v/v) solvent mixture to yield 15 fractions (Fr. 1-15). Fr. 8 was dissolved in DMSO, recrystallized, and the residue was concentrated and separated using silica gel chromatography, followed by gradient elution with CHCl₃-MeOH to yield six subfractions (S1-S5). Subfraction S-5 was further purified using a Sephadex LH-20 column with CHCl₃-MeOH elution. The resulting fraction was crystallized to yield a compound (300 mg). The structure elucidation of the isolated compound was done using NMR and mass spectral data. ¹H, ¹³C, and 2D NMR spectral data sets were recorded using a Bruker Avance-III 400 MHz spectrometer (Bruker, Zürich, Switzerland), while mass spectroscopy (MS) data of the compound were recorded on a Waters Q-ToF Premier mass spectrometer (Waters, Milford, MA, USA) using a direct inlet system.

Cell line and culture

The mouse S180 cell line was purchased from the Type Culture Collection Cell Bank of the Chinese Academy of Sciences (Shanghai, China) and grown in RPMI 1640 medium supplemented with 10% FBS, 1% GlutaMAX, and 25 mM HEPES buffer, maintained at 37°C in an atmosphere of 5% CO₂ in a humidified incubator (Thermo,

Waltham, MA, USA). Cells in the logarithmic growth stage were used for all experiments.

Animals

Adult male Kunming mice (4- to 6-week old) with a body weight of 18.0-22.0 g were purchased from the Experimental Animal Center of the Third Military Medical University in Chongqing, China (Animal License No. SCXK ZUN 2012-0011). The animals were housed in a controlled environment at a temperature of 22-25°C, with 50 ± 10% humidity and a 12-h light/dark cycle, and fed sterile pellets and water *ad libitum*. The animal study protocol was approved by the Zunyi Medical University Committee for the Control and Supervision of Experimental Animals. All experimental animals were acclimated for seven days before use.

Evaluation of antitumor activity *in vivo*

As described previously,¹² tumor cells were inoculated into the peritoneal cavity of healthy male Kunming mice under sterile conditions. The ivory-colored ascitic fluid of the inoculated mice was harvested after eight days and diluted 4-fold with sterile saline; 0.5 mL of this dilution was then passaged into the peritoneal cavity of another healthy mouse. After 10 days, the S180 ascitic tumor was harvested, washed twice with sterile saline, and suspended in sterile saline at a density of 1 × 10⁷ cells/mL. Then, 200 μ L of the tumor cell suspension was inoculated subcutaneously into the right groin of each mouse. When the tumor diameter reached approximately 5 mm (day 0), the tumor-bearing mice were randomly divided into five study groups of 16 mice each; these were the vehicle control (MG), CTX, high-dose helvolic acid (HA-H), low-dose helvolic acid (HA-L), and a combination of CTX and HA-L (CG) groups. HA-L and HA-H mice were intraperitoneally administered helvolic acid once daily at doses of 10 and 20 mg/kg, respectively, (0.2 mL per mouse) for 10 consecutive days. The helvolic acid was successively dissolved in 5% total volumes each of DMSO, Tween-80, and castor oil as isometric complex solubility promoters, and then finally made up with 85% of the total volume of saline. The CG (10 mg/kg helvolic acid and 20 mg/kg CTX, once daily), PG (20 mg/kg CTX once daily), and MG (treated with the helvolic acid vehicle) mice were treated using the same schedule.

During the experiments, the length and width of the tumors were measured using digital calipers and each mouse was also weighted once a day starting on day 5 after administration. The tumor volume (mm³) was calculated as the (length × width²)/2. Two independent experiments were performed for each treatment, with eight mice per group. On day 3 after the last drug administration, eight mice from each group were anesthetized, euthanized by cervical dislocation, and then weighed. Simultaneously, their solid tumors were quickly removed, weighed, fixed in 10% paraformaldehyde for at least 24 h, and then vacuum-embedded in paraffin. The remaining mice were allowed to live until they died a natural death, and their time of death was recorded and used

to calculate the median survival time (MST). The lifetime prolonging rate (LPR) of the tumor hosts was calculated as follows, based on the mortality of the mice: $MST = \Sigma$ survival time of each mouse in the group/the total number of mice; $LPR (\%) = (MST \text{ of treated group} / MST \text{ of control group}) \times 100$. The tumor inhibition ratio was calculated as follows: tumor inhibition ratio (%) = (average tumor weight of model group - average tumor weight of treatment group)/average tumor weight of control group $\times 100$.

Immune organ indices

After the mice had been euthanized, the thymus and spleen of each mouse were immediately removed, washed, and weighed. The immune organ indices were defined as the thymus or spleen weight, or both, relative to the total body weight, and calculated using the following formula: organ index (%) = organ weight/body weight $\times 100$.

Histomorphological analyses and immunohistochemical staining

The tumors and livers of three mice in each group were analyzed using H&E and immunohistochemical staining. As described previously,¹² all the tumors were washed with normal saline, fixed with 10% paraformaldehyde in phosphate-buffered saline (PBS), successively dehydrated in increasing concentrations of ethyl alcohol (75, 85, 95, and 100%), vacuum-embedded in paraffin, cut into 4- μ m-thick sections, and deparaffinized in histoclear clearing agent. The sections were subsequently H&E-stained and histomorphologically analyzed.

For the immunohistochemical staining, the sections were sequentially rehydrated with graded concentrations of alcohols (100, 90, and 70%) in water. Then, heat-induced epitope retrieval was performed by treating the sections with 10 mM citrate buffer (pH 6.0) and heating four times in a microwave oven at medium power once for 2 min. The endogenous tissue peroxidase activity was blocked by incubation with 3% hydrogen peroxide (H₂O₂) in methanol for 30 min at room temperature, followed by three washes in PBS. The non-specific binding was quenched with 50% normal goat blocking serum (Gene Tech, Shanghai, China) for 40 min. The sections were then incubated overnight at 4°C with primary rabbit anti-mouse monoclonal antibodies against β -catenin, PCNA, and cyclin D1 (1:100 in PBS). The sections were rinsed thrice with PBS (3 min each time) and then incubated at 37°C for 30 min with a peroxidase-conjugated goat anti-rabbit IgG secondary antibody. After washing thrice with PBS, immunoreactivity was visualized using 3,3'-diaminobenzidine as the chromogen, the sections were counterstained with hematoxylin, and then coverslipped. Finally, the stained sections were observed under a microscope and their brown-colored staining was scored using the Image-Pro Plus 6.0 (Media Cybernetics, Inc., Bethesda, MD, USA). The mean optical density was subsequently calculated. Appropriate positive and negative controls (without primary antibody) were included.

Statistical analysis

The data were expressed as the mean \pm the standard deviation. Statistical comparisons were performed by analysis of variance using the statistical package for the social sciences (SPSS) version 19.0, and a *P* value of <0.05 was considered statistically significant.

Results

Structure elucidation of the isolated compound

The compound was obtained as colorless needle crystals (MeOH) followed by both silica gel and Sephadex LH-20 column chromatography. The molecular formula C₃₃H₄₄O₈ was fixed by HR-ESI-MS (neg.) at *m/z* 567.2938 [M-H]⁻. The ¹H NMR data (500 MHz, CDCl₃) obtained from the compound are 7.31 (1H, d, *J* = 10.0 Hz, H-1), 5.87 (1H, d, *J* = 9.8 Hz, H-2), 2.78 (1H, m, H-4), 2.27 (1H, d, *J* = 12.6 Hz, H-5), 5.24 (1H, s, H-6), 2.11 (3H, s, 6-OCOCH₃), 2.63 (1H, dd, *J* = 10.4 Hz, 12.7 Hz, H-9), 1.57 (1H, m, H-11), 1.81 (1H, m, H-12), 2.59 (1H, br d, *J* = 6.6 Hz, H-13), 2.27 (2H, d, *J* = 12.6 Hz, H-15), 5.89 (1H, s, H-16), 1.94 (3H, s, 16-OCOCH₃), 0.93 (3H, s, H-18), 1.45 (3H, s, H-19), 2.46 (2H, m, H-22), 2.14 (1H, m, H-23), 5.11 (1H, m, H-24), 1.69 (3H, s, H-25), 1.61 (3H, s, H-27), 1.28 (3H, d, *J* = 6.9 Hz, H-28), 1.18 (3H, s, H-29). The ¹³C NMR data (125 MHz, CDCl₃) obtained from the compound is 157.3(C-1), 127.8(C-2), 201.4(C-3), 40.4(C-4), 47.2(C-5), 73.8(C-6), 168.9(6-OCOCH₃), 20.7(6-OCOCH₃), 208.8(C-7), 52.7(C-8), 41.7(C-9), 38.2(C-10), 23.9(C-11), 25.9(C-12), 49.4(C-13), 46.6(C-14), 40.6(C-15), 73.5(C-16), 170.3(16-OCOCH₃), 20.5(16-OCOCH₃), 147.6(C-17), 17.9(C-18), 27.5(C-19), 130.5(C-20), 174.2(C-21), 28.6(C-22), 28.3(C-23), 122.8(C-24), 132.9(C-25), 17.8(C-26), 25.7(C-27), 13.1(C-28), 18.4(C-29). Both ¹H and ¹³C NMR data revealed that the structure of the compound matches that of the known nortriterpenoid helvolic acid and were consistent with previous many reports.¹⁻³ Thus, the isolated compound was assigned as the helvolic acid, whose chemical structure is shown in Figure 1(a).

Antitumor efficacy of helvolic acid alone or combined with CTX in tumor-bearing mice

We examined the antitumor efficacy of helvolic acid in murine S180 tumor-bearing male Kunming mice treated with MG, CTX, HA-H, HA-L, and CG groups. As shown in Figure 1(b), (c) and (f), the individual and combined treatment groups (HA-L, HA-H, and CG) did not exhibit significant body weight loss, as compared to the MG. However, in contrast to the *in vitro* data, helvolic acid alone produced only slight inhibition of tumor growth *in vivo*. Figure 1(d) shows the tumor volume over the course of treatment and tumors in the HA-L mice continued to grow progressively, as did those in the MG. Furthermore, analysis of the tumor tissue weights in the euthanized mice hardly showed any inhibition of tumor growth at the tested doses of helvolic acid (Figure 1(b) and (e)). Surprisingly, the combined helvolic acid and CTX treatment significantly reduced the externally measured tumor volume (Figure 1(d)). The mean tumor size of the CG was the smallest of the four drug treatment groups; their mean tumor

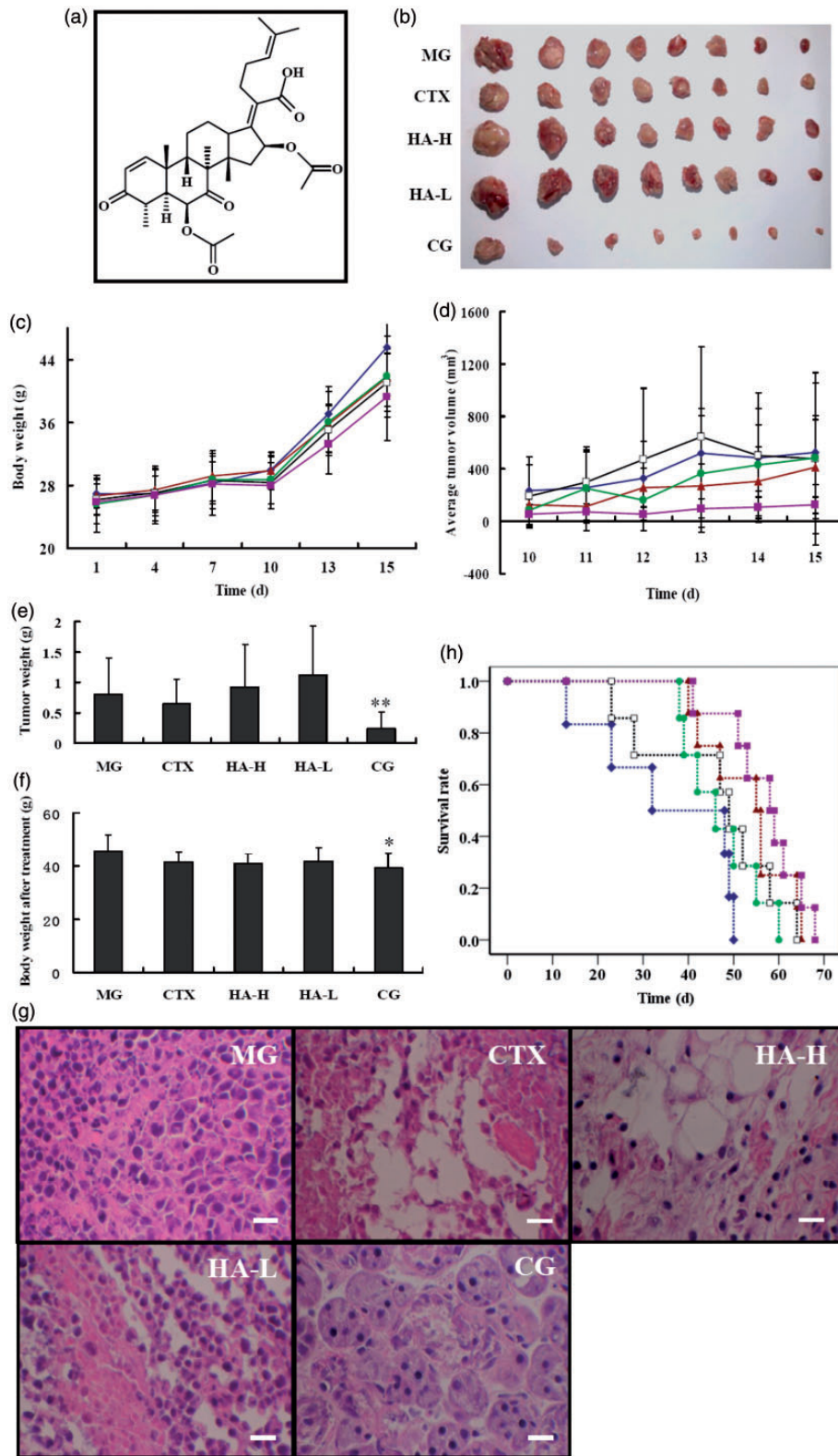


Figure 1 Antitumor effects of helvolic acid (HA) and cyclophosphamide (CTX) in a mouse tumor model. (a) Chemical structure of helvolic acid. (b) Tumors from the indicated treatment groups at euthanasia. (c) Body weights and (d) tumor sizes after tumor inoculation. (e) Tumor weights and (f) body weights at euthanasia. (g) Hematoxylin and eosin-stained tumor tissue sections from the indicated groups. (h) Survival of tumor-burdened mice after the indicated treatments. (◆) MG; (▲) CTX; (□) HA-H; (●) HA-L; (■) CG; MG, model vehicle control group; CTX, CTX-treated group; HA-H, high-dose helvolic acid; HA-L, low-dose helvolic acid; CG, combination of CTX + HA-L group. * $P < 0.05$ and ** $P < 0.01$ vs. MG. Scale bar = 50 μm

Table 1 The survival rates of male S180 tumor-bearing Kunming mice

Groups	Median survival time (day)	Lifetime prolonging rate (%)
MG	35.83 ± 15.64	–
CTX	53.13 ± 9.38**	48.26 ± 26.11
HA-H	46.85 ± 15.09	27.97 ± 42.12
HA-L	47.14 ± 8.30	31.56 ± 23.15
CG	57.00 ± 8.57**	59.07 ± 23.91

MG: model vehicle control group; CTX: CTX-treated group; HA-H: high-dose helvolic acid; HA-L: low-dose helvolic acid; CG: combination of CTX+HA-L group. ** $P < 0.01$ vs. MG, $n = 8$.

weight was one-third to one-fifth of those of the other groups. The tumor weights of the CG mice were significantly lower than those of the MG animals were, but no significant difference was observed between the tumor weights of the MG and CTX-treated mice (Figure 1(e)). Tumor weight decreased by over 70% in the CG, corresponding to a 3.6-fold greater effect than that observed in the CTX-treated mice. Therefore, helvolic acid and CTX induced a considerable synergistic antitumor effect.

To elucidate the antitumor effects of these treatments further, we analyzed tumor tissues of mice from each group histopathologically using hematoxylin and eosin (H&E) staining. Compared with the MG, the HA-L mice showed no evidence of an effect on the tumor structure, except for the presence of a looser cell arrangement (Figure 1(g)). However, CTX induced changes in the tumor cell arrangement, with evidence of numerous necrotic cells and cytoplasmic structures, and similar results were observed in the HA-H mice. Interestingly, the CG mice showed a significant inhibition of the division of the tumor cells, which mostly presented as round cells with a multinuclear structure. In addition, the survival periods of the tumor-burdened mice were investigated in this study (Figure 1(h) and Table 1). All drug treatment groups showed a MST that was prolonged by 11–22 days, as compared with the MG. This was particularly apparent in the CG mice, which achieved the highest survival time of 57.00 ± 8.57 days; this was a statistically significant difference ($P < 0.01$) from the MG group. The LPR of the CG was 59.1%. However, because of the large variations between animals, there was no statistically significant difference in the LPR rates of the study groups (Table 1).

Effect of helvolic acid alone or combined with CTX on immune organs and liver tissue in tumor-bearing mice

The immune system in the tumor-bearing mouse model may influence tumor development and progression. Therefore, we analyzed the immune organ indices, as shown in Figure 2(a) and (b). The antitumor drug CTX, which is an immunosuppressant, induced a slightly lower spleen index than that observed in the MG mice. Interestingly, helvolic acid significantly raised the thymus and spleen indices at both of the doses tested in the present study. The immune organ indices of the CG were higher than that of the MG, although this difference was not significant, and were lower

than those of the HA-L and HA-H groups were, perhaps owing to CTX-mediated immunosuppressive effects. H&E staining of the liver tissue did not identify any liver toxicity in any of the treatment groups (Figure 2(c)).

Effect of helvolic acid alone or combined with CTX on the expression of Wnt/ β -catenin pathway-associated proteins in tumor-bearing mice

The Wnt/ β -catenin signaling pathway plays a pivotal role in cancer pathogenesis and progression, modulating tumor initiation and growth, cell senescence and death, differentiation, and metastasis. We investigated a central component of this pathway, β -catenin, and two downstream response components, PCNA and cyclin D1, using immunohistochemistry (Figure 3). Enhanced protein expression of β -catenin (brown) was observed in the cell cytoplasm and nuclei of tumor tissue of the MG mice (Figure 3(a)). There was also enhanced expression of β -catenin in the tumor cell nuclei of the HA-L and HA-H animals. The CG and CTX group both showed a substantially decreased expression of β -catenin, as compared with the MG ($P < 0.01$, Figure 3(b)). In addition, the expression of β -catenin in the CG was significantly lower than it was in the PG ($P < 0.05$, Figure 3(b)). Similarly, the CG mice showed significantly lower expression of PCNA and cyclin D1, as compared with the MG mice ($P < 0.01$, Figure 3(b)). Although this group showed the strongest inhibitory effect, the HA-H mice also showed marked reductions in the levels of PCNA ($P < 0.05$) and cyclin D1 ($P < 0.01$), as compared with the MG (Figure 3(b)).

Discussion

Helvolic acid, which was discovered to be an effective antibacterial agent and has been used since the 1940s, has been of considerable interest to researchers worldwide. The major purpose of this study was to investigate whether helvolic acid has the potential to be developed as a candidate antitumor agent, based on its isolation from the active antitumor fraction of *C. taii* and its potent *in vitro* activity against cancer cells. Although our results showed that it had no direct antitumor effects *in vivo*, helvolic acid unexpectedly exhibited a significant potential of the synergistic antitumor effects with the well-known chemotherapeutic drug, CTX, with few side-effects. In addition, it markedly inhibited the expression of β -catenin, a central component of the Wnt signaling pathway, and of two downstream proteins – PCNA and cyclin D1.

In our *in vivo* test, the S180 tumor size and weight were not affected by treatment with helvolic acid alone. However, the combined treatment with helvolic acid and CTX significantly decreased these parameters as compared with the other study controls. Furthermore, H&E staining revealed some necrotic and lysed areas in the tumor tissues of the HA-H group, while minimal necrosis and lysis were present in the HA-L group. Survival time was also extended by more than 11 days in the HA-L and HA-H groups, with an LPR of approximately 30% (Table 1). These results appeared to indicate that helvolic acid alone had a weak cytotoxic effect on tumor cells. In the CTX group, H&E

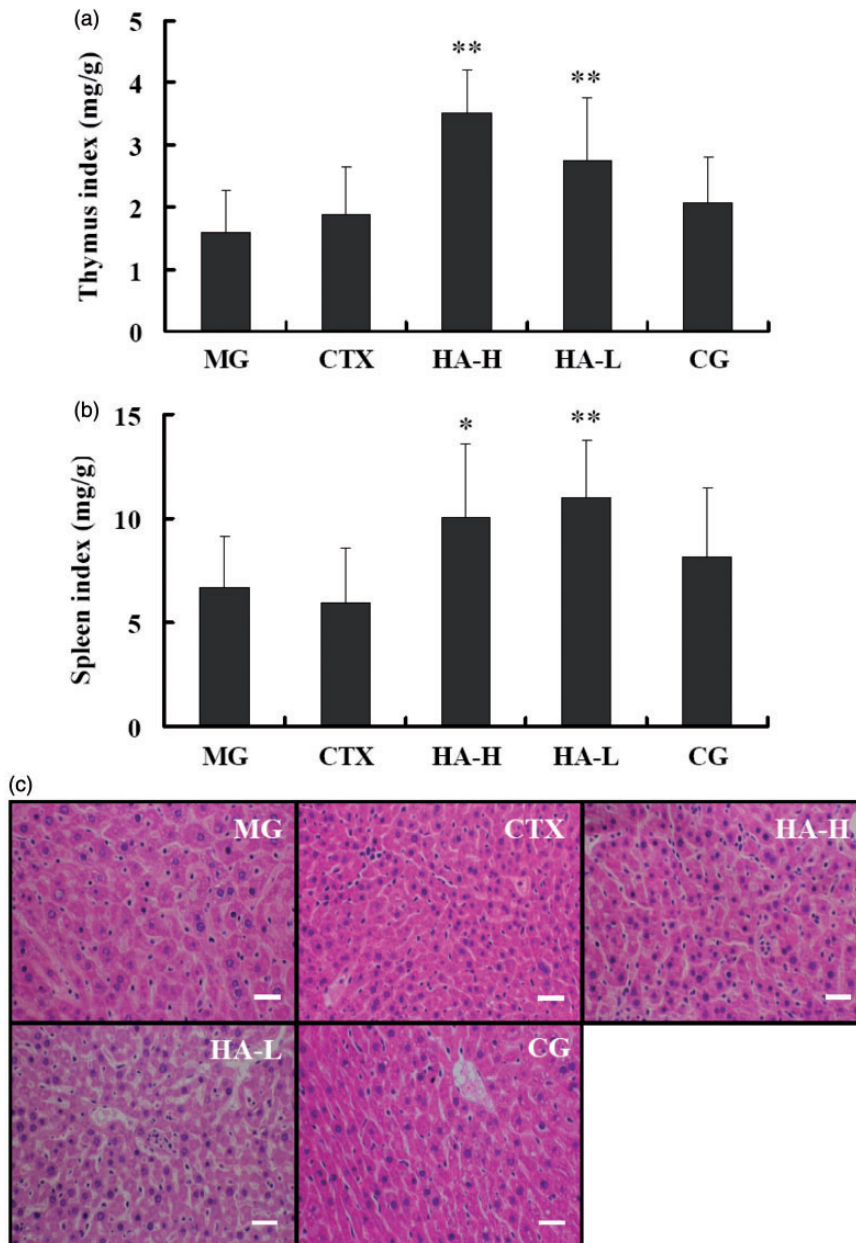


Figure 2 Effects of the indicated treatments on immune organ indices and liver tissue in tumor-burdened mice. (a) Thymus and (b) spleen indices. (c) Hematoxylin and eosin-stained liver tissue from the indicated groups. MG: model vehicle control group; CTX: CTX-treated group; HA-H: high-dose helvolic acid; HA-L: low-dose helvolic acid; CG: combination of CTX + HA-L group. * $P < 0.05$ and ** $P < 0.01$ vs. MG. Scale bar = 100 μm

staining revealed substantially larger areas of necrosis and lysis than those observed in either helvolic acid-treated group. Similar to previous reports,^{12,19} CTX at a dose of 20 mg/kg exhibited good tumoricidal activity against S180 tumor. Furthermore, it also showed markedly prolonged survival time in S180 tumor-bearing mice. As we know, CTX is a well-characterized alkylating agent that is one of the most frequently used clinical chemotherapeutic agents. Previous studies showed that CTX not only induced cancer cell death owing to its cytotoxicity, but also enhanced the host antitumor immune response; this was associated with a reduction of the number of CD11b⁺Gr1⁺ myeloid-derived suppressor cells, elimination of regulatory T cells (Tregs),

induction of T_H17 cells, and promotion of interferon γ and T_H17 cytokine production.^{20,21} The relative importance of immune potentiation and direct cytotoxicity for the antitumor effects of CTX depends on the dose administered. Low doses of CTX contribute to antitumor immunity while high doses act solely by inducing cytotoxicity. For example, Ghiringhelli *et al.*²² reported that administration of 25–30 mg/kg CTX depleted CD4⁺CD25⁺ T cells in rats and delayed the growth of colon carcinomas. Similarly, Motoyoshi *et al.*²³ showed that low-dose CTX (20 mg/kg), but not high-dose CTX (200 mg/kg), selectively suppressed CD4⁺CD25⁺ T cell numbers, while sparing conventional CD4⁺ and CD8⁺ T cells and preventing murine hepatoma

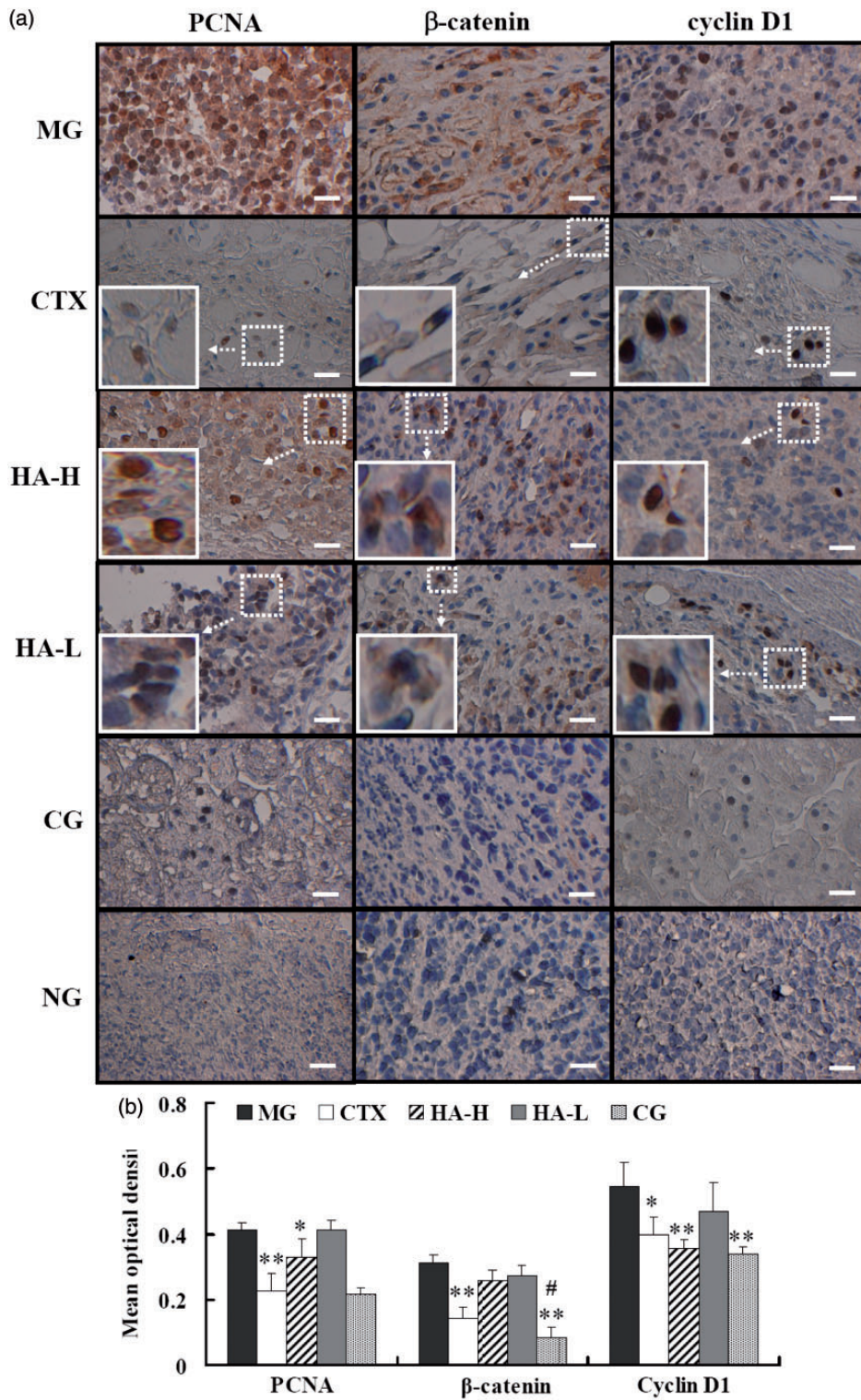


Figure 3 Effects of the indicated treatments on Wnt/ β -catenin pathway proteins in tumor-burdened mice. (a) Immunohistochemical staining for the indicated proteins in tumor tissue. (b) Mean optical densities of the indicated protein signals. MG: model vehicle control group; CTX: CTX-treated group; HA-H: high-dose helvolic acid; HA-L: low-dose helvolic acid; CG: combination of CTX + HA-L group. NG: indicates tissue from the MG mice, processed in the absence of primary antibody as a negative control. * $P < 0.05$ and ** $P < 0.01$ vs. MG; # $P < 0.05$ vs. PG. Scale bar = 50 μ m

growth. Therefore, low-dose CTX can potentiate antitumor immunity in mouse models via depletion of CD4⁺CD25⁺ T-reg cells, and reduction of immunosuppressive cytokines,^{24,25} whereas high doses of CTX inhibit the antitumor immune response via bone marrow suppression.^{16,26} In this

study, CTX (20 mg/kg) alone could result in a slight increase and decrease for thymus index, and spleen index, respectively, whereas the thymus is closely associated with T-cells. Accordingly, our data are an indirect evidence that low-dose CTX (20 mg/kg) caused cancer cell death in this

immunocompetent mouse model via an underlying immunomodulatory mechanism.

Interestingly, the combined CTX and helvolic acid treatment not only promoted a considerable increase in immune organ indices, as compared with both the MG and CTX-treated group, but also significantly inhibited tumor growth. Furthermore, while it did not cause substantial cancer cell necrosis and lysis, it induced cell growth arrest by inhibiting cell division (Figure 1(g)), indicating non-classical characteristics that likely differed from those of CTX. Recent study reported that anethole and high dose CTX (100 mg/kg) singly resulted in apoptosis, and necrosis, respectively, in S180 tumor-bearing mice, but there was a distinct shift in the population of cells from necrosis to apoptosis in the combinatorial treatment of anethole and CTX, and use of anethole was instrumental in reducing the side-effects including myelosuppression, hepatotoxicity, and urotoxicity of CTX treatment.¹⁶ As described above, helvolic acid significantly increased the immune organ indices at both tested doses. Therefore, the primary effect of helvolic acid in the combination therapy might be associated with immune system activation, and the effects of helvolic acid and CTX co-administration likely reflected antitumor immune responses. However, the mechanism underlying the effects of the combination therapy may be not the same as those underlying the actions of CTX or helvolic acid alone, based on the histological results obtained. Recently, some chemotherapeutic agents have been demonstrated to stimulate the immune system, resulting in host antitumor immune responses that contribute to their clinical efficacy.²¹ Certainly, the role of helvolic acid in the combination therapy requires further investigation.

The Wnt signaling pathway has been identified in numerous tumor types, implicated in tumorigenesis and cancer progression, and has become a valid new target for cancer drug development.²⁷ In the present immunohistochemical study, substantial reductions in the expression of the central component, β -catenin, and of two downstream effectors, PCNA and cyclin D1, were identified in the CTX group; this effect was even more pronounced in the CG. Immunohistochemical staining for cytoplasmic or nuclear β -catenin can indicate Wnt signaling activity, with predominant staining of nuclear β -catenin suggesting Wnt/ β -catenin pathway activation, which results in the interaction of β -catenin with T-cell factor/lymphoid enhancer factor transcription factors.²⁸ The MG mice showed increased cytoplasmic and nuclear accumulation of β -catenin, while the other treatment groups showed a lower nuclear β -catenin level than that observed in the MG animals. In particular, the CG showed negligible nuclear β -catenin expression. These findings suggested that the combination treatment might have potentially inhibited Wnt/ β -catenin signaling. In addition, the HA-L and HA-H groups exhibited decreased levels of these components, with a significantly lower PCNA and cyclin D1 expression in the mice treated with the high dose, as compared to that observed in the MG.

In summary, the present study was the first to demonstrate that the antitumor activities of helvolic acid and CTX were markedly enhanced when they were used in combination, and that CTX-induced immunosuppression was

alleviated by helvolic acid. Further studies are necessary to investigate the non-classical molecular mechanisms involved in the cell growth arrest and death induced by this combination, which were likely mediated via inhibition of cell division. In addition, it would be worth exploring the potential synergistic antitumor efficacy of helvolic acid in combination with other chemotherapeutic agents. Finally, our findings suggest that there might be a clinical benefit in using a combination of helvolic acid and CTX to treat patients with cancer, and for this reason, this study warrants further investigation along this line towards real clinical application.

Authors' contributions: JHX, GYL, RML, DXC, and JJZ conceived and designed the experiments; YZ performed the experiments; JHX, YZ, RML, and LTZ analyzed the data; RML and XGL contributed reagents/materials/analysis tools; JHX drafted the manuscript. All the authors approved the final manuscript.

ACKNOWLEDGMENTS

The authors are grateful for the financial support of the National Natural Science Foundation of China (No. 81260278; 81060260), the Guizhou High-Level Innovative Talent Support Program (No. QKH-RC-20154028), and the Program for Innovative Research Team in Guizhou Province (No. QKH-RCTD-20134035).

DECLARATION OF CONFLICTING INTERESTS

The author(s) declared no potential conflicts of interest with respect to the research, authorship, and/or publication of this article.

REFERENCES

- Ratnaweera PB, Williams DE, De Silva ED, Wijesundera RLC, Dalisay DS, Andersen RJ. Helvolic acid, an antibacterial nortriterpenoid from a fungal endophyte, *Xylaria* sp. of orchid *Anoetochilus setaceus* endemic to Sri Lanka. *Mycology* 2014;5: 23–8
- Zhao J, Mou Y, Shan T, Li Y, Lu S, Zhou L. Preparative separation of helvolic acid from the endophytic fungus *Pichia guilliermondii* Ppf9 by high-speed counter-current chromatography. *World J Microbiol Biotechnol* 2012;28:835–40
- Lee SY, Kinoshita H, Ihara F, Igarashi Y, Nihira T. Identification of novel derivative of helvolic acid from *Metarhizium anisopliae* grown in medium with insect component. *J Biosci Bioeng* 2008;105:476–80
- Li Y, Song YC, Liu JY, Ma YM, Tan RX. Anti-*Helicobacter pylori* substances from endophytic fungal cultures. *World J Microbiol Biotechnol* 2005;21:553–8
- Qin L, Li B, Guan J, Zhang G. *In vitro* synergistic antibacterial activities of helvolic acid on multi-drug resistant *Staphylococcus aureus*. *Nat Prod Res* 2009;23:309–18
- De Vendittis E, De Paola B, Gogliettino MA, Adinolfi BS, Fiengo A, Duvold T, Bocchini V. Fusidic and helvolic acid inhibition of elongation factor 2 from the archaeon *Sulfolobus solfataricus*. *Biochemistry* 2002;41:14879–84
- Singkaravanit S, Kinoshita H, Ihara F, Nihira T. Cloning and functional analysis of the second geranylgeranyl diphosphate synthase gene influencing helvolic acid biosynthesis in *Metarhizium anisopliae*. *Appl Microbiol Biotechnol* 2010;87:1077–88

8. Chen C, Pan WD, Xiao JH, Liang GY. Investigations on chemical constituents of methanolic extract from *Penicillium jiangxiense* (*Cordyceps jiangxiensis*). *Chin J Exp Trad Med Formulae* 2011;**17**:97–101
9. Li XG, Pan WD, Zhang XJ, Xiao JH. Antitumor chemical entities of the mycelia of medicinal mushroom *Cordyceps taii* from Guizhou. *J Chin Med Mat* 2015;**38**:2083–6
10. Xiao JH, Xiao DM, Sun ZH, Xiong Q, Liang ZQ, Zhong JJ. Chemical compositions and antimicrobial property of three edible and medicinal *Cordyceps* species. *J Food Agr Environ* 2009;**7**:91–100
11. Xiao DM, Xiao JH, Zhang ZM, Sun ZH. Antimicrobial potential of *Metarhizium taii* *in vitro*. *J Chin Med Mat* 2010;**33**:952–7
12. Liu RM, Zhang XJ, Liang GY, Yang YF, Zhong JJ, Xiao JH. Antitumor and antimetastatic activities of chloroform extract of medicinal mushroom *Cordyceps taii* in mouse models. *BMC Complement Altern Med* 2015;**15**:216
13. Dou Y, Xiao JH, Xia XX, Zhong JJ. Effect of oxygen supply on biomass and helvolic acid production in submerged fermentation of *Cordyceps taii*. *Biochem Eng J* 2013;**81**:73–9
14. Huang XH, Xiong PC, Xiong CM, Cai YL, Wei AH, Wang JP, Liang XF, Ruan JL. *In vitro* and *in vivo* antitumor activity of *Macrothelypteris torresiana* and its acute/subacute oral toxicity. *Phytomedicine* 2010;**17**:930–4
15. Britto ACS, de Oliveira AC, Henriques RM, Cardoso GMB, Bomfim DS, Carvalho AA, Moraes MO, Pessoa C, Pinheiro MLB, Costa EV, Bezerra DP. *In vitro* and *in vivo* antitumor effects of the essential oil from the leaves of *Guatteria friesiana*. *Planta Med* 2012;**78**:409–14
16. Jana S, Patra K, Mukherjee G, Bhattacharjee S, Mandal DP. Antitumor potential of anethole singly and in combination with cyclophosphamide in murine Sarcoma-180 transplantable tumor model. *RSC Adv* 2015;**5**:56549–59
17. Cao J, Hou D, Lu J, Zhu L, Zhang P, Zhou N, Chen K. Anti-tumor activity of exopolysaccharide from *Rhizopus nigricans* Ehrenb on S180 tumor-bearing mice. *Bioorg Med Chem Lett* 2016;**26**:2098–104
18. Li XG, Pan WD, Luo HY, Liu RM, Xiao JH, Zhong JJ. New cytochalasins from medicinal macrofungus *Cordyceps taii* and their inhibitory activities against human cancer cells. *Bioorg Med Chem Lett* 2015;**25**:1823–6
19. Wang J, Chen S, Xu S, Yu X, Ma D, Hu X, Cao X. *In vivo* induction of apoptosis by fucoxanthin, a marine carotenoid, associated with down-regulating STAT3/EGFR signaling in sarcoma 180 (S180) xenograft-bearing mice. *Mar Drugs* 2012;**10**:2055–68
20. Chen X, Wakefield LM, Oppenheim JJ. Synergistic antitumor effects of a TGF β inhibitor and cyclophosphamide. *Oncol Immunology* 2014;**3**: e28247
21. Apetoh L, Ladoire S, Coukos G, Ghiringhelli F. Combining immunotherapy and anticancer agents: The right path to achieve cancer cure? *Ann Oncol* 2015;**26**:1813–23
22. Ghiringhelli F, Larmonier N, Schmitt E, Parcellier A, Cathelin D, Garrido C, Chauffert B, Solary E, Bonnotte B, Martin F. CD4⁺CD25⁺ regulatory T cells suppress tumor immunity but are sensitive to cyclophosphamide which allows immunotherapy of established tumors to be curative. *Eur J Immunol* 2004;**34**:336–44
23. Motoyoshi Y, Kaminoda K, Saitoh O, Hamasaki K, Nakao K, Ishii N, Nagayama Y, Eguchi K. Different mechanisms for anti-tumor effects of low- and high-dose cyclophosphamide. *Oncol Rep* 2006;**16**:141–6
24. Lutsiak ME, Semnani RT, de Pascalis R, Kashmiri SV, Schlom J, Sabzevari H. Inhibition of CD4⁺25⁺ T regulatory cell function implicated in enhanced immune response by low-dose cyclophosphamide. *Blood* 2005;**105**:2862–8
25. Castano AP, Mroz P, Wu MX, Hamblin MR. Photodynamic therapy plus low-dose cyclophosphamide generates antitumor immunity in a mouse model. *Proc Natl Acad Sci USA* 2008;**105**:5495–500
26. Le DT, Jaffee EM. Regulatory T-cell modulation using cyclophosphamide in vaccine approaches: a current perspective. *Cancer Res* 2012;**72**:3439–44
27. Tai D, Wells K, Arcaroli J, Vanderbilt C, Aisner DL, Messersmith WA, Lieu CH. Targeting the Wnt signaling pathway in cancer therapeutics. *Oncologist* 2015;**20**:1189–98
28. Anastas JN, Moon RT. WNT signalling pathways as therapeutic targets in cancer. *Nat Rev Cancer* 2013;**13**:11–26

(Received February 18, 2016, Accepted May 12, 2016)